Steady-state dendritic crystal growth

David A. Kessler
Department of Physics, University of Michigan, Ann Arbor, Michigan 48109

Joel Koplik and Herbert Levine
Schlumberger-Doll Research, Old Quarry Road, Ridgefield, Connecticut 06877-4108
(Received 2 December 1985)

We study the problem of velocity and shape selection in the growth of dendritic crystals. We demonstrate that the presence of surface tension destroys the Ivantsov family of solutions at all but a single velocity. This occurs at all undercoolings and for both two-dimensional and axisymmetric three-dimensional dendrites. The lack of a continuous family of solutions is due to a mismatch of terms exponentially small in velocity, in agreement with the mechanism of "microscopic solvability" previously derived for geometrical growth models.

I. INTRODUCTION

Dendritic crystal growth has long served as a standard example of pattern formation in nonequilibrium systems. Dendritic growth occurs in a variety of physical contexts ranging from solidification to electrochemical deposition to growth from vapor.[1,2] Strikingly, the shape and velocity of the dendrite arms are unique, experimentally *reproducible* functions of the applied forces, independent of the initial conditions.[3] Understanding the workings of such systems is a necessary step for progress in the field of dynamics far from equilibrium.

The simplest example of this phenomenon is crystal growth in solidification from a pure supercooled melt. Here, we may safely assume that the rate of growth is controlled by the diffusion of the released heat of fusion away from the solid-liquid interface. The first approach to this problem, by Ivantsov[4] and Horvay and Cahn,[5] modeled the heat flow by a macroscopic transport equation which coupled to the interface through the local equilibrium assumption that at the interface temperature equaled the bulk melting temperature. This assumption produces an infinite continuous family of allowed parabolic shapes for the dendritic main branch, with arbitrary tip velocity. Subsequently, several authors[2] added additional postulates in an attempt to fix a unique shape in accord with experiment.

All of the work based upon the original Ivantsov analysis must introduce a new length scale in order to specify the pattern. It was recognized quite early that surface tension γ gives rise to a capillary length $d_0 = \gamma / L$ (L is the latent heat per unit volume), which modifies the previous analyses via the Gibbs-Thomson[6] boundary condition: the temperature at the interface equals $T_M(1 - d_0 \kappa)$, where T_M is the bulk melting temperature and κ the local curvature. There remained the question of how d_0 actually does determine the shape. In the "maximum velocity" approach, for example, the shape is related to a fastest-growing spherical approximation to the tip shape, while in the "marginal stability" hypothesis the velocity is such that the tip is neutrally stable. In both

cases the selection issue involves the dynamical choice of one of the continuous family of zero-surface tension solutions. Whereas the maximum velocity can be ruled out experimentally, marginal stability has been fairly successful as a rule of thumb for estimating growth velocity, and in particular, gave rise to a useful scaling relation between tip velocity and tip radius for small undercooling.

The purpose of this paper is to show that the supposition that both these approaches build upon, that there is a continuous family of allowed steady-state shapes, is not correct. We will show that at any finite value of d_0, there is a unique steady-state solution. The continuous family disappears when we impose a solvability condition brought about by the inclusion of surface tension. Remarkably, this solvability condition fails to be satisfied by terms which are exponentially small in the velocity. This accounts for the failure of the perturbative methods used in the past.

These results have been presaged by developments in related systems over the past few years. First, the introduction of simplified models of interfacial dynamics[7,8] led to the idea that solvability conditions could determine unique shapes.[9,10] Next, heuristic arguments were given that the Ivantsov family would be critically sensitive to the introduction of surface tension.[11] Finally, there was a realization that the selection of finger width for the analogous Saffman-Taylor[12] problem could be understood along similar lines.[13] These developments suggested the paradigm of "microscopic solvability" for pattern formation in interfacial motion. It is this hypothesis that we verify in this paper for dendritic crystal growth. Some of our results, for the limit of small undercooling, have been presented elsewhere.[14]

The outline of this paper is as follows. In Sec. II, we review the integral formulation of the steady-state dendrite equation in two dimensions. We derive the leading corrections to the Ivantsov parabola asymptotically far from the tip region. In Sec. III we describe our numerical procedure and present the results of our calculations. We show that at all undercoolings, crystal anisotropy is necessary to obtain finite velocities. We further show that

surface-tension effects are exponentially small, so that the actual selected solution is experimentally indistinguishable from the Ivantsov solution *at the correct velocity*. In Sec. IV, we extend the analysis to axisymmetric dendrites in three dimensions, with similar results. Section V summarizes our current state of knowledge and indicates some future directions for research.

II. TWO-DIMENSIONAL STEADY-STATE EQUATION

We wish to study the evolution of a solid-liquid interface controlled by thermal diffusion. As described by Langer,[2] the governing equations for the temperature T can be taken as

$$D\nabla^2 T = \frac{\partial T}{\partial t} ,$$

$$T(\mathbf{x}_I(s)) = T_M(1 - d_0\kappa(s)\{1 - \epsilon\cos[4\theta(s)]\}) , \quad (1)$$

$$c_p D[(\hat{\mathbf{n}}\cdot\nabla T)_l - (\hat{\mathbf{n}}\cdot\nabla T)_s] = L\mathbf{v}(s)\cdot\hat{\mathbf{n}} ,$$

where d_0 is the capillary length, L is the latent heat per volume, and c_p and D are, respectively, the specific heat and thermal diffusivity, assumed for simplicity to be equal in the solid and liquid. We have assumed that the surface tension has a fourfold anisotropy, being smallest when the angle $\theta(s)$ between the normal and the crystal

axis is a multiple of $\pi/2$. The interface is given by $\mathbf{x}_I(s)$, has arc length s, curvature $\kappa(s)$, and normal velocity $\hat{\mathbf{n}}\cdot\mathbf{v}(s)$. The last equation relates the discontinuity in the temperature gradient going from liquid to solid to the rate of heat release. Finally, the temperature approaches $T_M - \Delta$ (T_M is the melting temperature and Δ the undercooling) at large distances from the interface.

Because the temperature enters linearly in the above equations and its boundary values are fixed, it can be explicitly determined via an integral representation, viz.,

$$T(\mathbf{x}) = T_M - \Delta + \int ds'dt' G(\mathbf{x} - \mathbf{x}(s',t'), t - t')v_n(s',t') ,$$

$$(2)$$

where v_n is the normal velocity, G is the Green's function of the diffusion equation,

$$G(\mathbf{x},t) = \frac{1}{4\pi Dt}\exp\left[-\frac{\mathbf{x}^2}{4Dt}\right] .$$

Assuming a steady-state solution moving in the $\hat{\mathbf{y}}$ direction,

$$\mathbf{x}(s',t') = \mathbf{x}(s') - v\hat{\mathbf{n}}_y(t - t') . \quad (3)$$

We can integrate over t' to find

$$T(\mathbf{x}) = T_M - \Delta + \frac{vL}{2\pi c_p D}\int dx' K_0((v/2D)\{(x-x')^2 + [y - y(x')]^2\}^{1/2})e^{(v/2D)[y(x')-y]} ,$$

where K_0 is a Bessel function.

Finally, we evaluate this expression at the interface and rescale lengths by $v/2D$. We arrive at the final equation

$$\tilde{\Delta} - \tilde{v}\kappa\{1 - \epsilon\cos[4\theta(\mathbf{x})]\}$$

$$= \frac{1}{\pi}\int dx' K_0([(x-x')^2 + (y-y')^2]^{1/2})e^{y-y'} , \quad (4)$$

where

$$\tilde{v} = \frac{vd_0}{2D}\frac{T_M}{L/c_p}, \quad \tilde{\Delta} = \frac{\Delta}{L/c_p} .$$

Equation (4) and its later generalization to three dimensions form the basis of the analysis which follows.

In the absence of capillarity, i.e., at $\gamma = \tilde{v} = 0$, one can easily verify that $y_I = -x^2/2p$ solves the above equation, provided $\Delta = \sqrt{\pi p}\,e^p\text{erfc}(\sqrt{p})$. Note that p is the Peclet number, since it is the tip radius in length units $v/2D$, and that as $p\to\infty$, $\Delta\to 1$, which is the required undercooling for a planar interface. This Ivantsov[4] parabola solution is valid at large x, since the resulting curvature vanishes there, and we now wish to determine the rate at which the true solution approaches it. On the left-hand side of (4),

$$-\tilde{v}\kappa[1 - \epsilon\cos(4\theta)] \sim -\tilde{v}p^2/x^3(1 - \epsilon)$$

at large x. We assume that

$$y(x) = -x^2/2p + a/x \quad (5)$$

and verify that it can be chosen to give a similar term on the right-hand side of the steady-state equation.

Let us substitute (5) into the integral in (4). First,

$$d \equiv [(x-x')^2 + (y-y')^2]^{1/2}$$

$$\cong d_0 + \frac{a}{2p}\frac{(x^2-x'^2)(x-x')}{xx'd_0} ,$$

where

$$d_0^2 = (x-x')^2 + \frac{1}{4p^2}(x^2-x'^2)^2 .$$

This gives a term

$$\frac{a}{\pi}\int_{-\infty}^{\infty} dx'\left[K_0(d_0)\left[\frac{x-x'}{xx'}\right]\right.$$

$$\left. - \frac{K_1(d_0)}{2p}\frac{x^2-x'^2}{xx'd_0}(x-x')\right]e^{(x'^2-x^2)/2p} .$$

It can be shown that the leading contribution to the integral comes from the region $x' < x$. We can therefore use the asymptotic forms for the Bessel functions at large arguments. A short computation leads to the final expression for the coefficient of a

$$\frac{\sqrt{p}}{x^3\sqrt{\pi}}\int_0^{\infty} dz\frac{e^{-pz}}{\sqrt{z}}\left[\frac{2zp^2}{1-z} - \frac{p}{1-z}\right] , \quad (6)$$

where we employed the change of variables $z = (x - x')/(x + x')$. Equating expression (6) to the left-hand side of (4) determines a as a function of the Peclet number. Note that as $p \to 0$, (6) vanishes more slowly than p^2, requiring $a \to 0$. This agrees with the $p = 0$ result of Pelcé and Pomeau[15] that $y = -x^2/2p + O(1/x \ln x)$ in the small undercooling limit. Finally, it is amusing to note the above integral can also be written as the analytic continuation

$$2 \frac{\partial}{\partial(1/p)} [\sqrt{-\pi p} \, e^{-p} \, \mathrm{erfc}(\sqrt{-p})] \,,$$

a form which can be explicitly verified by doing an expansion around the planar interface limit.

Our strategy will be to search numerically for steady-state solutions which approach the Ivantsov parabola with the above perturbative correction. We will then see if these solutions satisfy Eq. (4) all the way up to the tip region. The next section describes our numerical procedure.

III. NUMERICAL RESULTS

We now look for numerical solutions of the steady-state equations. Our approach is based on a method devised by Vanden-Broeck[16] for the Saffman-Taylor viscous fingering problem.[12,13] The idea is to relax the integral equation (4) at the tip, allowing for a possible cusp in the interface. With this freedom, solutions exist for all values of $\bar{v}$ for any Δ. We then solve an auxiliary equation requiring the cusp magnitude (the discontinuity in dy/dx at the tip) to vanish, to determine the actual selected $\bar{v}$.

To proceed, we discretize the x range using the parametrization $x_j = \tan(\pi j/2N)$, $j = 0, 1, \ldots, N-1$. The steady-state integral equation then becomes a coupled set of $N-1$ nonlinear equations for the N unknowns $y(x_j)$. We require that y approach $-x^2/2p + a/x$ at large x, fixing $y(N-1)$. We then use a standard Newton's iteration routine to converge to the shape. We typically use values of N up to 100, and observe that the results converge quadratically. The key result of the computation is the cusp magnitude $f(\bar{v},p)$.

In Fig. 1, we have plotted $\ln[-f(\bar{v})]$ for the case of $p = 0.25$, corresponding to an undercooling $\tilde{\Delta} = 0.54$. At zero anisotropy, there are no solutions at all because f is negative for all $\bar{v}$. The functional dependence of f is consistent with the form $f \sim \exp[-C(p)/(\bar{v})^{1/2}]$, for all values of p. This result explains why the solvability condition is absent in an asymptotic expansion in powers of $\bar{v}$ and why, therefore, one can calculate a steady-state shape correction[17] without encountering any inconsistency. We will discuss this point further in the concluding section.

At any finite anisotropy, Fig. 1 shows that there does exist a velocity $\bar{v}^*$ at which a steady-state solution is possible. In Fig. 2, we plot $\bar{v}^*/p^2$ versus Peclet number at several values of the anisotropy. Simple scaling arguments[15] as well as a calculation performed at the zero Peclet number limit[14] suggest that at small p, $\bar{v}^* \sim g(\epsilon)p^2$. Our data is consistent with this result and shows how the velocity deviates from the scaling as Peclet number is increased. Note that this is just the scaling law obtained
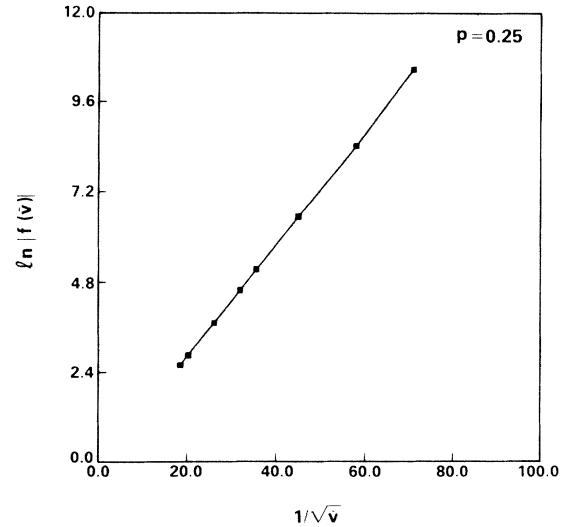
FIG. 1. Cusp magnitude versus velocity at $p = 0.25$.

from the marginal stability hypothesis,[2] here arising with no extraneous assumptions.

In Fig. 3, we have plotted the actual steady-state shape $y - y_I$ for the "typical" case of $p = 0.1$, $\epsilon = 0.05$. The deviation of this exact steady-state solution from the Ivantsov solution at the selected value $\bar{v}^* = 6 \times 10^{-5}$ is extremely small. This, of course, is a consequence of the fact that the dimensionless parameter $\sigma^* = v^*/p^2$ is quite small. An equivalent way of saying this is to note that the actual tip radius is much larger than the capillary length which is therefore a small perturbation. This important feature of our solvability mechanism is connected to the fact that at $\epsilon = 0$, only $\bar{v}^* = 0$ is allowed. Therefore, at small but nonzero anisotropy, $\bar{v}^* \sim \epsilon^\alpha$. Our data suggests that $1 \leq \alpha(p) \leq 1.5$, at small p, and it decreases slowly as p is increased.
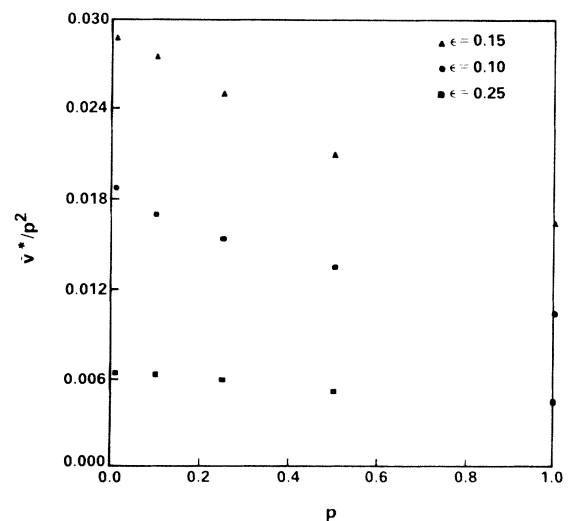
FIG. 2. Selected velocity versus p at several values of anisotropy.
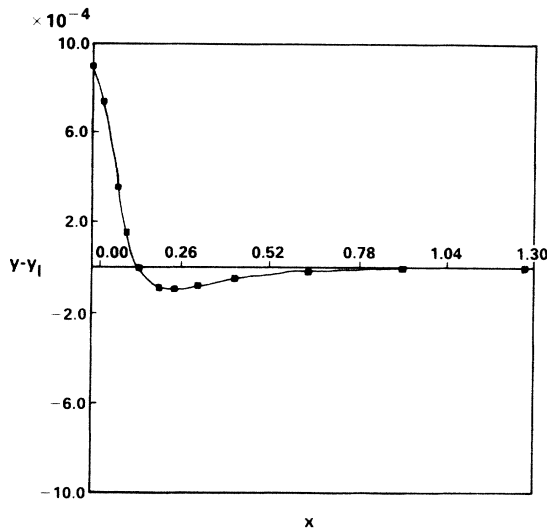
FIG. 3. Steady-state shape correction $y - y_I$, for $p = 0.1$ and $\epsilon = 0.05$.

vability condition at nonzero $\tilde{v}$. We will describe our method for obtaining this result and explain the generalization to nonaxisymmetric shapes which will be presented elsewhere.

We start again from Eq. (1) where the interface is now characterized by arc length at fixed azimuthal angle ϕ, and the angle ϕ. In the case of steady-state propagation, we can derive the integral representation

$$T(r,y) = T_M - \Delta + \frac{vL}{2\pi D c_p}$$
$$\times \int_0^\infty r' \, dr' \int_0^{2\pi} d\phi \frac{1}{d} e^{-d/l + (y' - y)/l} ,$$

where

$$d = [r^2 + r'^2 - 2rr' \cos\phi + (y' - y)^2]^{1/2}$$

and the thermal length $l = v/2D$. Rescaling all lengths by l and evaluating the temperature at the interface gives rise to the three-dimensional shape equation

$$\tilde{\Delta} - \tilde{v}\kappa = \frac{1}{2\pi} \int \int r' \, dr' \, d\phi \frac{e^{-d}}{d} e^{(y' - y)} . \tag{7}$$

One can check that with $\tilde{v} = 0$, the paraboloid of revolution $y = -r^2/2p$ satisfies (7) if the Peclet number p is related to the undercooling through the three-dimensional Ivantsov relation $\tilde{\Delta} = -p^p \text{Ei}(-p)$, where Ei is the exponential integral function.

To proceed, we need to understand the rate at which $y(r)$ approaches the Ivantsov result as we move away from the tail. The three-dimensional curvature asymptotically becomes

$$-\tilde{v}\kappa = \frac{-\tilde{v}}{r} + O\left[\frac{1}{r^3}\right] .$$

This suggests that the rate of approach in three dimensions will be much slower than that in two.

We assume that

$$y = -r^2/2P + ar + b \ln r + O\left[\frac{1}{r}\right] \tag{8}$$

and substitute this into the integral equation. Consider first the leading term, proportional to a. Expanding both the exponentials and the denominator, we find the expression

Before proceeding to three dimensions, we would like to emphasize again the fundamental simplicity of our approach. All one need do is to set up the integro-differential equation for interfacial shape and find solutions with an allowed cusp singularity. Convergence to this solution is extremely rapid with quadratic convergence in the number of discretization points. Complications to the above "simplest" model such as unequal diffusivities in the two phases, additional diffusion due to solute impurities, and the incorporation of interfacial kinetics through an interfacial undercooling are all easy to treat. Even the introduction of finite walls (growth inside a capillary tube) offers no problems in principle. This will be discussed in detail in a subsequent publication.

IV. THREE-DIMENSIONAL AXISYMMETRIC SOLUTIONS

We now extend our analysis to the case of axisymmetric dendrites in three dimensions. Unfortunately, the assumption of axisymmetry restricts our study to the case of no crystal anisotropy. As we might expect (based on the two-dimensional results), there are no solutions to the sol-

$$\frac{a}{2\pi} \int \int r' \, dr' \, d\phi \frac{e^{(r^2 - r'^2)/2p}}{d_0} e^{-d_0} \left[\frac{r - r'}{[(r^2 - r'^2)/2p]^2} - \frac{(r - r')}{(r^2 - r'^2/2p)} \frac{2p^2(r^2 + r'^2 - 2rr' \cos\phi)}{(r^2 - r'^2)^2} \right] ,$$

with

$$d_0^2 = r^2 + r'^2 - 2rr' \cos\phi + \left[\frac{r^2 - r'^2}{2p}\right]^2 .$$

The leading contribution to the integral becomes $r' < r$,

and from keeping only the leading two terms in d_0

$$\frac{r^2 - r'^2}{2p} - d_0 \cong -p\left[\frac{r^2 + r'^2 - 2rr' \cos\phi}{r^2 - r'^2}\right] .$$

We can now perform the angular integrals in terms of

Bessel functions. The final result, upon introducing the change of variable $q = (r - r')/(r + r')$, is

$$\frac{A_0}{r} \equiv \frac{1}{2r} \int \frac{dq}{q^2} e^{-pq} p^2 (1-q)$$

$$\times \{ I_1(z) e^{-z} [p(1-q^2)]$$

$$+ I_0(z) e^{-z} [2q - p(1+q^2)] \} , \qquad (9)$$

with $z = p(1-q^2)/2q$. The leading correction is then $a = -\tilde{v}/A_0$. We can check that as $p \to 0$, $a \to 0$, in agree-

ment with the analysis of Ref. 15 that at $p = 0$, $y - y_I \sim O(r/\ln r)$.

It is now a tedious but simple matter to extend the computation of the integral so as to evaluate the $1/r^2$ pieces. The most important point to notice is that all of the corrections due to keeping more terms in the expansion of d_0 as well as due to the range $r > r'$ fall faster than $1/r^2$; the only pieces which contribute are a linear term in b and a quadratic term in a. The final result for the integral to this order in $1/r$ is

$$(bA_1 + a^2 A_2)/r^2 ,$$

where

$$A_1 = \int_0^\infty \frac{dq}{q^2} e^{-pq} \frac{-1}{4q} p^2 (1-q)(1+q)^2 \ln \left| \frac{1-q}{1+q} \right| \left\{ I_1(z) e^{-z} p(1-q) + I_0(z) e^{-z} \left[\frac{2q}{1+q} - \frac{p(1+q)}{2} \left[1 + \frac{(1-q)^2}{(1+q)^2} \right] \right] \right\}$$

and   (10)

$$A_2 = \int \frac{dq}{4q^3} (1-q^2) e^{-pq} \{ I_1(z) e^{-z} [3pq(1-q^2) - (1-q^4)p^2] + I_0(z) e^{-z} [p^2(1+q^4) - 4pq(1+q^2) + 4q^2] \} .$$

All of these integrals can be evaluated numerically for arbitrary p and compared to a separately derived asymptotic expansion value for p very large.[15] Finally, matching this to the left-hand side of the equation clearly requires choosing $b = -A_2 a^2 / A_1$.

We now parametrize the interface by the variable z, defined via

$$y(r) = -r^2/2p + ar + b \ln r + z .$$

We again discretize the r variable as in two dimensions and solve the resulting nonlinear system of equations. In Fig. 4, we plot the cusp magnitude against $\tilde{v}$ for Peclet number 0.1. We find no solution other than $\tilde{v}^* = 0$ and an essential singularity in f as $\tilde{v} \to 0$. This remains true
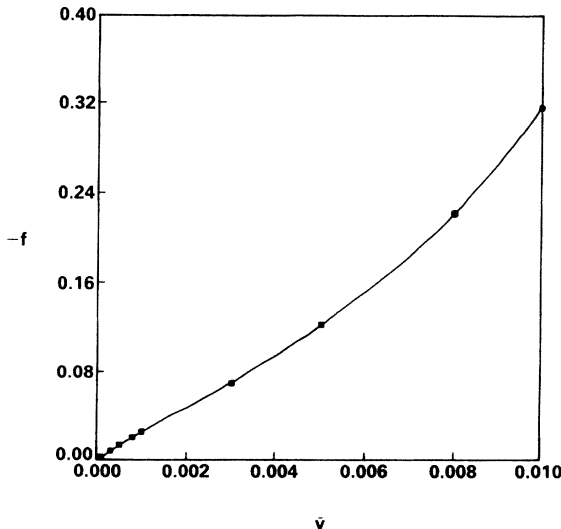
FIG. 4. Cusp magnitude versus velocity for three-dimensional axisymmetric solutions.

for all values of p. This is exactly the same as we found earlier in two dimensions and agrees with the idea that anisotropy is necessary for obtaining steady-state solutions.

We briefly sketch the generalizations necessary to accommodate finite anisotropy and hence nonaxisymmetric shapes. The integral equation is modified by the multiplication of the curvature by an angular dependence characteristic of the crystal structure; e.g., for a cubic anisotropy

$$\tilde{v}_\kappa \to \tilde{v}_\kappa [1 - \epsilon \cos(4\theta)\cos(4\phi)] .$$

Asymptotically, the left-hand side approaches $(-\tilde{v}/r)[1 - \epsilon \cos(4\phi)]$. We therefore assume

$$y = \frac{-r^2}{2p} + r[a_0 + a_1 \cos(4\phi)] + b_0 \ln r$$

$$+ b_1 \cos(4\phi) + b_2 \cos(8\phi)$$

and evaluate all the resulting integrals. Finally, the interface is parametrized as

$$z(r,\phi) \equiv \sum_{m=0}^{m_{max}} \cos 4m \phi z_m (r)$$

and we would solve for the unknowns by evaluating the equation at the collocation points

$$\phi_m = \frac{\pi m}{2(m_{max} + 1)} .$$

Aside from the large increase in computation time, the implementation of this method is straightforward.

V. DISCUSSION

Over the past few years, we and others have developed a theory of microscopic solvability to account for the unique patterns seen in diffusion-controlled interfacial

evolution. This approach posits a three-step approach to the determination of the final shape.

(a) Look for steady-state shapes in the *absence* of any microscopic dynamics. This will, in general, give rise to a continuous family of possible shapes, typified here by the Ivantsov solutions in both two and three dimensions.

(b) Solve the full steady-state equation, requiring that the solution approach the previously found shapes far from the tip region. This will introduce, via terms essentially singular in the microscopic parameter, a solvability condition which has at most a discrete set of solutions.

(c) Compute the stability of the resulting steady-state shape with respect to both linear and nonlinear perturbations.

This paper has shown how to carry out step (b) for the case of dendritic crystal growth. We found that there was indeed a solvability condition whenever we include finite-surface tension and that it determines a unique solution. Furthermore, we showed that $\epsilon = 0$ is a critical point, completely analogous to the $\lambda = \frac{1}{2}$ limit of the Saffman-Taylor finger problem. Because of this, the physical systems such as succinonitrile[3] which have small anisotropy, will have $\tilde{v}^*$ small. This means that the actual pattern will be experimentally indistinguishable from the Ivantsov

solution at $\tilde{v}^*$. The only remnant of the microscopic dynamics is to *select* one of the Ivantsov parabolas.

We have not yet tackled the stability analysis of this steady-state solution. However, we expect that as the selected velocity is decreased, there will eventually be a transition to disordered growth, i.e., tips will split rather than sidebranch. This has been seen experimentally[17] in growth from solution, in electrochemical deposition,[18] and in a hydrodynamic analogue of crystal growth.[19] We still need to understand the mechanism whereby sidebranching is the mode of operation over a large range of system parameters, unlike what occurs in local growth models.[7,8,20]

Finally, we would like to point out that much work needs to be done to find an analytic approach powerful enough to see solvability. There has been much progress on this issue for local models, either by WKB methods[21] or by more exact analysis.[22] The small value of $\tilde{v}^*$, related to the distance to the critical point $\epsilon = 0$, means that the idea of linearizing[21,22] the solvability condition is possibly a good method to approach this problem. This gives rise to a linear inhomogeneous integro-differential equation which is currently under investigation.

After completion of this manuscript, we became aware of the independent work of D. Meiron (private communication) which comes to the same conclusions regarding velocity selection of two-dimensional dendrites.

[1] For a recent review, see D. Kessler, J. Koplik, and H. Levine, *Proceedings of the Symposium on the Chemistry and Physics of Composite Media,* edited by M. Tomkiewicz and P. N. Sen (Electrochemical Society, New York, 1985).

[2] J. S. Langer, Rev. Mod. Phys. **52**, 1 (1980).

[3] M. E. Glicksman, Mater. Sci. Eng. **65**, 45 (1984).

[4] G. P. Ivantsov, Dokl. Akad. Nauk. SSSR **58**, 567 (1947).

[5] G. Horvay and J. W. Cahn, Acta Metall. **9**, 695 (1965).

[6] D. P. Woodruff, *The Solid-Liquid Interface* (Cambridge University Press, Cambridge, 1973).

[7] R. C. Brower, D. Kessler, J. Koplik, and H. Levine, Phys. Rev. Lett. **51**, 1111 (1983); Phys. Rev. A **29**, 1335 (1984); D. Kessler, J. Koplik, and H. Levine, *ibid.* **30**, 3161 (1984).

[8] E. Ben-Jacob, N. Goldenfeld, J. S. Langer, and G. Schön, Phys. Rev. Lett. **51**, 1930 (1983); Phys. Rev. A **29**, 330 (1984).

[9] D. Kessler, J. Koplik, and H. Levine, Phys. Rev. A **31**, 1712 (1985).

[10] E. Ben Jacob, N. Goldenfeld, G. Kotliar, and J. S. Langer, Phys. Rev. Lett. **53**, 2110 (1984).

[11] R, C. Brower, D. Kessler, J. Koplik, and H. Levine, Scr. Metall. **18**, 463 (1984); see also B. Caroli, C. Caroli, B. Roulet, and J. S. Langer, Phys. Rev. A **33**, 442 (1986).

[12] P. G. Saffman and G. I. Taylor, Proc. R. Soc. London A **245**, 312 (1958).

[13] D. Kessler and H. Levine, Phys. Rev. A **32**, 1930 (1985); **33**, 2621 (1986); **33**, 2634 (1986).

[14] D. Kessler and H. Levine (unpublished).

[15] P. Pelcé and Y. Pomeau (unpublished).

[16] J. M. Vanden-Broeck, Phys. Fluids **26**, 2033 (1983).

[17] A. Hanjo, S. Ohta, and Y. Sawada, Phys. Rev. Lett. **55**, 841 (1985).

[18] Y. Sawada, A. Dougherty, and J. Gollub (unpublished); D. Grier, E. Ben-Jacob, R. Clarke, and L. M. Sander (unpublished).

[19] E. Ben-Jacob, R. Godbey, N. D. Goldenfeld, J. Koplik, H. Levine, T. Mueller, and L. M. Sander, Phys. Rev. Lett. **55**, 1315 (1985).

[20] H. Müller-Krumbhaar, G. Goldbeck, and Y. Saito, Proceedings of the Seminar on Crystal Morphology and Growth Units, Yamagata, Japan, 1985.

[21] J. S. Langer, Phys. Rev. A **33**, 435 (1986).

[22] M. Kruskal and H. Segur (unpublished); R. Dashen, D. Kessler, H. Levine, and R. Savit (unpublished).